International Journal of Nanomedicine

Dovepress
open access to scientific and medical research

Open Access Full Text Article

ORIGINAL RESEARCH

Polyacrylate/nanosilica causes pleural and pericardial effusion, and pulmonary fibrosis and granuloma in rats similar to those observed in exposed workers

This article was published in the following Dove Press journal:
International Journal of Nanomedicine
18 April 2016
Number of times this article has been viewed

Xiaoli Zhu[1]
Wen Cao[2]
Bing Chang[3]
Linyuan Zhang[3]
Peihuan Qiao[3]
Xue Li[4]
Lifang Si[5]
Yingmei Niu[1]
Yuguo Song[1]

[1]Department of Occupational Medicine and Clinical Toxicology, Beijing Chaoyang Hospital, Capital Medical University, Beijing, People's Republic of China; [2]Department of Ultrasound, Beijing Chaoyang Hospital, Capital Medical University, Beijing, People's Republic of China; [3]Department of Toxicology, National Institute for Occupational Health and Poison Control, China CDC, Beijing, People's Republic of China; [4]Department of Pathology, Beijing Chaoyang Hospital, Capital Medical University, Beijing, People's Republic of China; [5]Department of Radiology, Beijing Chaoyang Hospital, Capital Medical University, Beijing, People's Republic of China

Abstract: Nanomaterials offer great benefit as well as potential damage to humans. Workers exposed to polyacrylate coatings have pleural effusion, pericardial effusion, and pulmonary fibrosis and granuloma, which are thought to be related to the high exposure to nanomaterials in the coatings. The study aimed to determine whether polyacrylate/silica nanoparticles cause similar toxicity in rats, as observed in exposed workers. Ninety male Wistar rats were randomly divided into five groups with 18 rats in each group. The groups included the saline control group, another control group of polyacrylate only, and low-, intermediate-, and high-dose groups of polyacrylate/nanosilica with concentrations of 3.125, 6.25, and 12.5 mg/kg. Seventy-five rats for the 1-week study were terminated for scheduled necropsy at 24 hours, 3 days, and 7 days postintratracheal instillation. The remaining 15 rats (three males/group) had repeated ultrasound and chest computed tomography examinations in a 2-week study to observe the pleural and pericardial effusion and pulmonary toxicity. We found that polyacrylate/nanosilica resulted in pleural and pericardial effusions, where nanosilica was isolated and detected. Effusion occurred on day 3 and day 5 post-administration of nanocomposites in the 6.25 and 12.5 mg/kg groups, it gradually rose to a maximum on days 7–10 and then slowly decreased and disappeared on day 14. With an increase in polyacrylate/nanosilica concentrations, pleural effusion increased, as shown by ultrasonographic qualitative observations. Pulmonary fibrosis and granuloma were also observed in the high-dose polyacrylate/nanosilica group. Our study shows that polyacrylate/nanosilica results in specific toxicity presenting as pleural and pericardial effusion, as well as pulmonary fibrosis and granuloma, which are almost identical to results in reported patients. These results indicate the urgent need and importance of nanosafety and awareness of toxicity of polyacrylate/nanosilica.

Keywords: polyacrylate/nanosilica, pleural effusion, pericardial effusion, pulmonary fibrosis, granuloma

Introduction

Nanocomposites, defined as materials which have components mixed at the nanometer scale, are usually composed of two constituent materials, which are a matrix or host and a strengthening constituent called a nanofiller. Inorganic nanofillers that are used include metals, semiconductors, clay minerals, carbon-based materials, and other oxides, such as SiO_2. The choice of polymer matrix is also manifold depending on the applications that are generally divided into industrial plastics, conducting polymers, and transparent polymers, such as polymethyl methacrylate and polystyrene.[1]

Correspondence: Yuguo Song
Department of Occupational Medicine and Clinical Toxicology, Beijing Chaoyang Hospital, Capital Medical University, 8 Gongtinan Road, Chaoyang District, Beijing 100020, People's Republic of China
Tel +86 10 8523 1525
Fax +86 10 8523 1727
Email songrain123@hotmail.com

submit your manuscript | www.dovepress.com
Dovepress
http://dx.doi.org/10.2147/IJN.S102020

Because nanocomposites generate new superior properties and meet current and future demands in functional materials, they are widely used in numerous industrial applications, biomedical applications, and consumer products, such as paints and coating materials, plastic materials, latex, and adhesive materials.[2–5] In recent years, many countries have attached great importance to the development of new nanomaterials.

Polyacrylate/silica nanoparticles (PA/NPSi) are a nanosilica-containing nanocomposite that has broad applications in the paints and coatings industry. Because of the use of nanosilica, PA/NPSi have greatly improved the strength, chemical resistance, erosion and abrasion resistance, resistance to ultraviolet (UV) light, antifouling properties, abrasion and scratch resistance, aging-resistance, and climate-resistance of polymer materials. Additionally, PA/NPSi provide thermal stability and have super hydrophobic surface properties.[2,5–7] For coatings with microsilica, only hardness and abrasion resistance are slightly increased.[8] However, there are few studies on the toxicity of nanocomposites.

Importantly, we previously reported a group of patients who were exposed to nanomaterials (PA coatings), and they had pleural and pericardial effusion and pulmonary fibrosis and granuloma.[9] Two of these patients died and five were disabled after a long-term follow-up. Furthermore, NPSi have been isolated and detected in patients' pulmonary macrophages, pleural effusions, and microvessles.[10,11] We speculate that the patients' disease could be related to their high exposure to nanomaterials in the coatings.[9–11] The effects of PA/NPSi on animals, as well as the acute toxicities of PA/NPSi, are unknown. Therefore, this study aimed to determine the acute toxicities of PA/NPSi in rats. We examined the effects of PA/NPSi on pleural and pericardial effusion and pulmonary toxicity to investigate if they result in a similar toxicity to that of exposed workers.

Materials and methods

Laboratory apparatus and chemicals

An autoanalyzer (ADVIA 120; Siemens, Munich, Germany) and an automatic analyzer (7060; Hitachi Ltd., Tokyo, Japan) were used. A light microscope (Olympus BH2; Olympus Corporation, Tokyo, Japan) and transmission electron microscope (TEM, JEM-1400Plus; JEOL, Tokyo, Japan) were used for microscopy. The Acuson S2000 color ultrasonic diagnostic apparatus (Siemens) with linear array prober 9L4 was used. We performed computer tomography with the light speed-16 system (GE Healthcare Bio-Sciences Corp., Piscataway, NJ, USA).

PA (CAS:9003-21-8) was bought from Shanghai Zhixin chemical Ltd (Shanghai, People's Republic of China). PA/NPSi suspensions with mean nanosilica particle sizes of 20 nm (20±5 nm), similar in diameter to NPSi found in patients,[9,10] were made to order by Fudan University (Shanghai, People's Republic of China). The PA/NPSi nanocomposite was prepared by in situ emulsion polymerization.[12] The size and shape of NPSi were determined by TEM.

Animals

Adult male specific-pathogen-free Wistar rats, 4–6 weeks old, were purchased from Animal Center of Lianhelihua (Beijing, People's Republic of China). Rats (license, SCXK 2012-0001) were individually housed in a clean-grade animal room, at constant temperature (18°C–25°C) and humidity (45%–55%) with a 12 hour:12 hour light/dark cycle. The rats had free access to food and water. The rats were allowed to acclimatize for 7 days upon arrival prior to their use in the study and their body weights ranged from 180 to 220 g.

Processing of sampling and methods of administration

Freshly prepared PA/NPSi suspensions were diluted in normal saline with concentrations of 3.125, 6.25, and 12.5 mg/kg in a volume of 1 mL. PA/NPSi were administered to each rat in treatment groups. PA was ground and then mixed with normal saline to provide a concentration of 6.25 mg/kg for use in the control group, and another control group received only normal saline. Prior to use of the treatments, suspensions were sonicated for 20 minutes and vortexed briefly for 10 minutes. After anesthesia with ether, the rats were administered the PA/NPSi suspension by intratracheal instillation in a volume of 1 mL, with 0.5 mL to each lung. The control groups were treated with the same amount of saline or PA solution. All of the rats were checked daily for clinical signs and abnormal behavior and weighed every other day. Their body weight and clinic manifestations were recorded during the study period.

Experimental design

All of the experiments were conducted in accordance with the guidelines of Capital Medical University (Beijing, People's Republic of China) for the care and use of laboratory animals and with approval of the Animal Ethical Committee of Capital Medical University in the People's Republic of China. A total of 90 male Wistar rats were randomly divided into five groups with 18 rats in each group. The groups included a control group with physiological saline, another control group with

PA only, and low-, intermediate-, and high-dose groups of PA/NPSi with concentrations of 3.125, 6.25, and 12.5 mg/kg. The experiment included two parts. In the first part of a 1-week study, 75 rats were terminated for scheduled necropsy at 24 hours, 3 days, and 7 days postintratracheal instillation. The remaining 15 rats (three males/group) were included in the second part of the study, which included repeated ultrasound and chest computed tomography (CT) examinations in a 2-week study. We observed pleural and pericardial effusion and pulmonary toxicity. The remaining rats were sacrificed on day 14, and their lungs and pleural membranes were used for pathologic and TEM examinations.

Hematology analysis and blood biochemical assay

Blood samples were collected at necropsy from all rats from the abdominal aorta following euthanasia under 10% chloral hydrate (0.35 mL/100 g) and were placed in a vacutainer containing ethylenediaminetetraacetic acid. The following parameters were analyzed using an autoanalyzer: red blood cell count, white blood cell (WBC) count, hematocrit, hemoglobin concentration, mean corpuscular volume, mean corpuscular hemoglobin, mean corpuscular hemoglobin concentration, platelet count, reticulocyte count, and WBC differential count.

Blood samples were also centrifuged to obtain serum within 1 hour after collection. Serum biochemistry parameters were analyzed using an automatic analyzer. Liver function and nephrotoxicity were evaluated with serum levels of ALT, AST, GOT, LDH, total bilirubin, blood urea nitrogen, and creatinine.

Observing pleural effusions upon rats' dissection

After blood samples were collected from the rats' abdominal aorta, pleural cavities were carefully opened and we observed whether there was effusion, especially at both costophrenic angles. If effusion was present, we recorded its color and volume and collected it by sterile syringe for a routine examination. Effusion was also observed by TEM to determine whether there were NPSi and to examine the morphology of nanoparticles in the upper liquid after it was centrifuged at 300× *g* for 15 minutes.

Pathologic and TEM examinations of pleural membranes and lungs

After samples were collected, pleural membranes and the lungs were separately collected. They were briefly rinsed in ice-cold tissue mincing buffer and immediately fixed in 4% (v/v) formalin, embedded in paraffin blocks, then sliced into 5 μm sections. After hematoxylin and eosin staining or reticular fiber staining, the slides were observed and photographs were taken by two board-certified pathologists.

For transmission electron microscopy, a piece of pleural membrane and pulmonary fragments of 1 mm^3 (1×1×1 mm) were removed in randomly chosen areas of the lungs and infused immediately in 5% glutaraldehyde overnight. The samples were then treated according to the general protocols for transmission electron microscopy study. Tissue was then cut into ultrathin sections (500–800 A°) and stained with uranyl acetate and lead citrate. The samples were then examined at an accelerating voltage of 80 kV using TEM. Changes in cell morphology of pleural membrane and lung tissue samples, together with locations and distributions of NPSi, were observed and assessed.

Chest ultrasound examination for pleural and pericardial effusion

All remaining three rats in each group had ultrasound examinations performed on days 1, 3, 5, 7, 10, and 14 postintratracheal instillation. The rats were euthanized under 10% chloral hydrate (0.35 mL/100 g) as mentioned earlier. After shaving the hair using an electric shaver for rats and application of an ultrasound coupling gel to the skin, a probe was positioned on the chest or upper abdomen to detect the presence of pleural and/or pericardial effusion and possible damage of the liver and kidney. The rats' positions, when detected, were repeatedly changed in order to investigate the effusion.

Chest CT scanning

CT scanning of lungs was performed on day 7 and day14 postintratracheal instillation. The rats were anesthetized as mentioned earlier, placed on a plastic sheet in the prone position, and scanned using a commercial 64-channel CT. Scanning parameters were held constant at 64*0.625 mm detector configuration, 120 Kv (peak), and Mv 350 mAs. CT images were collected in axial, coronal, and sagittal views using a lung or chest window, and were further analyzed for regions of interest, including ground-glass opacity, lung fibrosis and pulmonary edema, especially pleural effusion. Shortly after CT scanning, the rats were sacrificed by exsanguination via the aorta. The lungs and pleural membranes were immediately excised and prepared as above for pathologic and TEM examinations.

Statistical analyses

Statistical analysis was performed with the SAS program (version 9.2; SAS Institute Inc., Cary, NC, USA). One-way analysis of variance (ANOVA) was employed on hematology and clinical chemistry among the groups. If results were significant, Dunnett's test was applied for multiple comparisons (significance level: 0.05 and 0.01). Values are shown as mean ± standard deviation. The volume of pleural and pericardial effusion was observed by ultrasonic examination and analyzed by the rank-sum test.

Results

Characterization of NPSi

The morphology and average size of NPSi were determined by TEM. TEM images showed that NPSi were mostly spherical and well dispersed. The mean size (standard deviation) of an individual nanoparticle is 20±5 nm (Figure 1A). A TEM image of nanoparticles stained with uranyl acetate and lead citrate is shown in Figure 1B.

General clinical manifestations

After 24 hours, clinical signs of toxicity in the intermediate- and high-dose groups were observed. Rats ate less food, moved and reacted less to irritants, and had facial edema and secretions from the canthus. Three days later, their body weights did not increase, but hair fluffiness was observed. By day 7, these signs gradually improved and body weight slowly increased. However, there was no significant change in body weight gain among groups during the first week. At day 14, in the three remaining rats in each group, the abnormal clinical signs had disappeared, but hair fluffiness was still observed, and body weight in the intermediate- and high-dose groups was significantly lower than that in the saline control group. Rats in the control groups and in the low-dose group appeared to be normal. No treatment-related mortality was observed in the rats.

Hematology and blood biochemical assay

Hematology analysis: the measured factors were within the normal range. There was no significant difference in hematological factors between the treatment groups and the saline control group. However, some rats in the high-dose group had high WBC counts (Table 1). Furthermore, rats in intermediate- and high-dose groups had monocytosis. They showed an elevated absolute monocyte count and neutropenia, with a decreased absolute neutrophil count, which are similar findings to those observed in exposed patients.

Biochemical analysis: on days 1, 3, and 7 postnanocomposite treatment, ALT, AST, GOT, LDH, and total bilirubin were all in the normal range. There were no significant differences in these parameters among the groups, although several rats in intermediate- and high-dose groups showed elevated levels of ALT and AST (Table 2). Additionally, changes in blood urea nitrogen and creatinine between controls and nanocomposite-administered groups were also assessed but were not significantly different to those of control rats (one-way ANOVA, $P>0.05$). No significant changes were observed in other biochemical indices after administration of PA/NPSi at all doses.

Necropsy and observation of pleural effusion

In the 3.25 mg/kg group, on day 1, there was slight hyperemia in the lungs without hemorrhagic spots, and the pleural

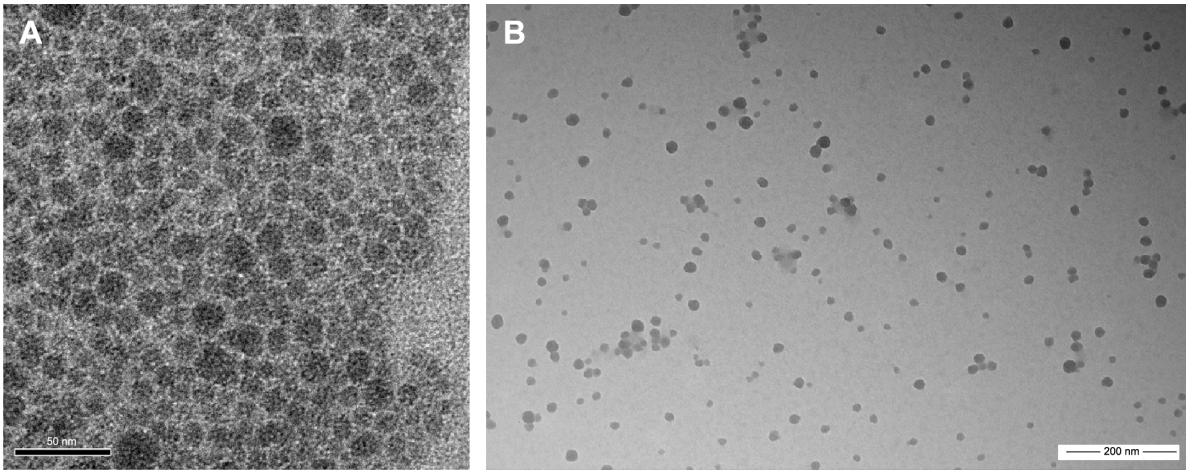

Figure 1 Silica nanoparticles in polyacrylate/nanosilica suspensions.
Notes: Silica nanoparticles in polyacrylate/silica nanocomposite (**A**) and nanoparticles stained with uranyl acetate and lead citrate (**B**).

Table 1 Hematology results of rats over a period of 7 days

Group	Number	24 hours				3 days				7 days			
		WBC ($\times 10^9$/L)	N ($\times 10^9$/L)	L ($\times 10^9$/L)	M ($\times 10^9$/L)	WBC ($\times 10^9$/L)	N ($\times 10^9$/L)	L ($\times 10^9$/L)	M ($\times 10^9$/L)	WBC ($\times 10^9$/L)	N ($\times 10^9$/L)	L ($\times 10^9$/L)	M ($\times 10^9$/L)
Control	5	4.29±1.87	0.94±0.47	2.41±1.53	0.14±0.08	4.26±2.63	0.83±0.41	4.61±2.37	0.16±0.55	4.21±2.40	0.78±0.46	3.45±1.97	0.14±0.20
Control/PA	5	3.91±1.52	0.79±0.57	1.86±0.78	0.16±0.10	4.45±2.92	0.93±0.46	3.27±1.70	0.15±0.21	4.36±1.74	1.48±0.85	3.01±1.39	0.18±0.13
3.125 mg/kg	5	3.86±2.52	0.88±0.56	2.62±1.64	0.19±0.47	4.66±2.57	1.17±0.64	3.42±2.09	0.17±0.13	5.21±2.78	1.09±0.67	2.27±1.38	0.07±0.06
6.25 mg/kg	5	4.43±2.62	1.03±0.45	3.80±2.37	0.19±0.05	5.08±3.21	0.89±0.43	3.29±1.29	0.27±0.18	3.99±2.09	0.94±0.53	2.30±1.54	0.21±0.16
12.5 mg/kg	5	5.37±2.62	0.70±0.38	3.88±1.99	0.24±0.21	5.47±2.60	0.88±0.40	2.45±1.71	0.31±0.18	4.16±1.48	1.03±0.81	2.19±1.12	0.22±0.11

Notes: All values represent the mean ± standard deviation. The measured factors were within the normal range. There were no significant differences in hematological factors between the treatment groups and the saline control group (all $P>0.05$). Some rats in the high-dose group had elevated WBCs with monocytosis and decreased absolute neutrophil counts.

Abbreviations: WBC, white blood cell; N, neutrophils; L, lymphocytes; M, monocytes; PA, polyacrylate.

membrane was smooth and transparent and broke easily when touched. No water in the pleural cavity was noted. On days 3 and 7, no water was observed in pleural cavity, but it was moist. In the 6.25 mg/kg group, on day 1, the lungs were swollen and distended and hyperemia with scattered hemorrhagic spots was observed. No water in the pleural cavity was noted, but it was moist. On days 3 and 7, the lungs were enlarged with a deepened color and old hemorrhagic spots. Amber or colorless pleural effusion was found and increased from 0.3–0.5 mL on day 3 to 0.4–0.8 mL on day 7. In the 12.5 mg/kg group, on day 1, damage to the lungs was similar to that in the 6.25 mg/kg group, but it was more severe with scattered or pieces of fresh hemorrhagic spots. The pleural membrane was adhesive and broke easily when touched, and the pleural cavity was moist, but no water was observed. On days 3 and 7, the lungs were enlarged with erosion of the thymus gland and pleura adhesion. Amber or colorless pleural effusion, which was much greater than that in the 6.25 mg/kg group, was found and increased from 0.4–0.8 mL on day 3 to 0.5–1.8 mL on day 7 (Figure 2A and B). On day 14, no water in the pleural space was noted in any of the groups, and pleural membranes in the 6.25 mg/kg and 12.5 mg/kg groups became stretchy and tough to break.

Routine examination and transmission electron microscopy observation of water in the chest

With dissection of rats, we found amber or colorless effusions in the intermediate- and high-dose groups on days 3 and 7 after administration. Chest fluid of several rats in the intermediate- and high-dose groups was analyzed. We observed that the total number of cells was 1,021±76/μL, the WBC count was 421±46/μL, monocytes were 78%–91%, polycytes were 9%–22%, specific density was 1.030–1.034, and the Rivalta test was positive (+). The effusions were exudates according to Light's criteria, similar to those in patients at the workplace.

With transmission electron microscopy, we found that the NPSi were dispersed in pleural effusion with clusters or individual form. The morphology and average size of nanoparticles were identical to that in suspensions. The nanoparticles were mostly spherical and well dispersed, and the average size of an individual nanoparticle was ~20 nm (Figure 3).

Pathologic examinations

Major histopathological changes were observed in lung tissues and pleural membranes of treated groups compared

Table 2 Serum biochemistry values of rats over a period of 7 days

Group	Number	24 hours					3 days	
		LDH (U/L)	ALT (U/L)	TBIL (μmol/L)	BUN (mmol/L)	Cr (μmol/L)	LDH (U/L)	ALT (U/L)
Control	5	367.29± 46.81	45.14±12.17	2.11±1.24	5.41±1.57	35.13±14.81	387.20±66.51	50.29±15.22
Control/PA	5	350.33± 62.53	48.29±15.56	2.86±1.78	5.86±1.78	31.44±9.16	470.33±201.53	55.21±12.76
3.125 mg/kg	5	421.84± 112.51	49.48±15.56	2.63±1.63	4.62±1.64	25.05±10.07	441.81±162.57	42.41±23.61
6.25 mg/kg	5	386.43± 122.66	57.23±20.45	2.18±1.37	5.80±2.31	30.71±15.92	436.43±182.36	40.51±18.51
12.5 mg/kg	5	436.31± 102.61	51.70±25.38	2.27±1.19	5.88±1.92	28.93±11.21	426.31±212.63	52.11±24.38

Notes: All values represent the mean ± standard deviation. They were all in the normal range. There were no significant differences in these parameters between the saline control group and the nanocomposite-administered groups (one-way ANOVA, all $P>0.05$).
Abbreviations: ANOVA, analysis of variance; TBIL, total bilirubin; BUN, blood urea nitrogen; Cr, creatinine; PA, polyacrylate.

with controls. Pathological changes of the lung and pleura and their severity in all treatment groups were shown to be dose-dependent after administration.

The control groups did not show any changes in appearance and micromorphology of the lung and pleural membrane at any time. On day 1, edema of alveoli, exudation in the alveolar space, increased alveolar macrophages, and interstitial infiltration of neutrophils were observed in all PA/NPSi treatment groups. Additionally, swelling of visceral and partietal pleura was also observed. With a rise of PA/NPSi concentrations, consolidation of pulmonary alveoli was observed in the high-dose group. Edema and lymphocytic infiltrations were found in the visceral and partietal pleura. On day 3, these changes persisted. On day 7, epithelial hyperplasia and early pulmonary fibrosis were noted, together with alveolar septal thickening and granuloma (Figure 4A–F). The reticular fiber staining showed that reticular fibers enwrapped granulation tissue, and they formed the circular structure of the granuloma (Figure 4G). Edema and lymphocytic infiltrations, as well as exudation with red blood cells and inflammatory cells in the visceral and partietal pleura, were observed. We also observed pleural thickening and interstitial fibrosis.

Transmission electron microscopy observations

At 1–7 days of administration of PA/NPSi, we observed alveolar edema, exudation in alveolar space with red blood cells and inflammatory cells, and swellings of organelles in alveolar cells at all doses of treatment. In the high-dose group, alveolar collapse or consolidation was observed. On day 7, there were a lot of collagen fibers in the lungs and the parietal pleural membrane in the high-dose group (Figure 5A and B). On day 14, in the low-dose group, alveolar septum was enlarged, and the pulmonary interstitium showed hyperplasia and slight fibrosis (Figure 5C and D). In the intermediate- and high-dose groups, pulmonary edema was still present, as well as exudation with red blood cells and inflammatory cells. We observed alveolar wall thickening, an enlarged alveolar septum and interstitial fibrosis, as well as increased number of monocytes and hyperplasia of type 2 alveolar epithelial cells and collagen fibers. Also, in the high-dose group, areas of pulmonary alveoli consolidation and hyperplasia of fibers were observed. The parietal pleura also showed fibrosis.

On days 7 and 14, NPSi were still found inside the cytoplasm and nucleus of macrophages or adhered to cell surface in lung tissue and scattered in some of the parietal

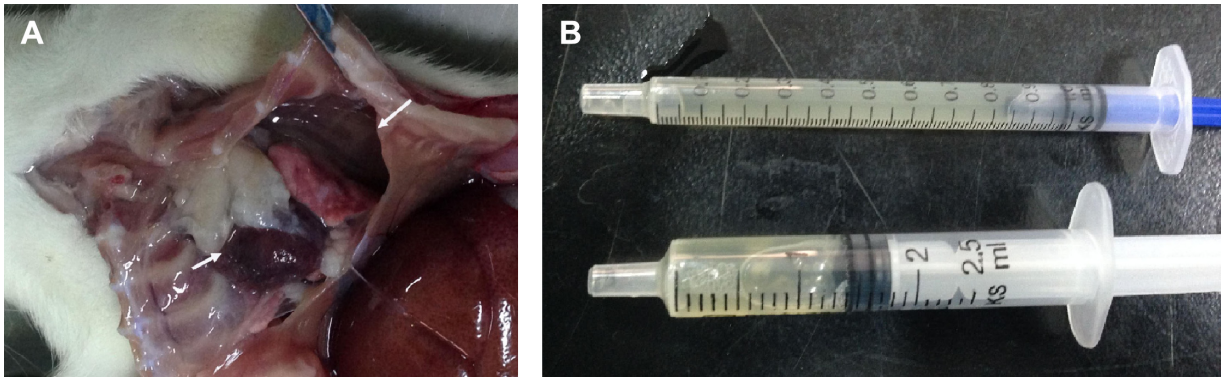

Figure 2 Pleural effusion was observed in a rat with approximately 1–1.8 mL in each pleural cavity.
Notes: (A) Pleural effusion in both pleural cavities in a rat. (**B**) Approximately 1 mL and 1.8 mL fluid in each pleural cavity.

			7 days				
TBIL (μmol/L)	BUN (mmol/L)	Cr (μmol/L)	LDH (U/L)	ALT (U/L)	TBIL (μmol/L)	BUN (mmol/L)	Cr (μmol/L)
2.01±0.93	4.91±3.37	32.10±9.28	418.36±116.12	41.21±20.24	2.06±1.03	5.45±1.07	30.14±12.20
1.96±0.88	5.27±1.72	35.43±11.17	450.31±101.53	51.22±21.71	1.86±0.76	6.01±1.32	33.18±9.13
2.02±1.14	5.42±2.19	35.03±14.04	491.80±261.50	46.45±17.62	2.12±1.04	6.27±1.35	31.07±10.06
2.80±1.07	6.09±1.22	30.97±11.02	506.43±190.31	50.54±16.53	2.18±0.67	5.80±1.74	40.07±14.06
2.35±0.99	5.45±1.78	26.19±16.14	436.35±112.61	56.11±28.31	2.38±0.99	6.19±1.18	28.12±12.11

pleural tissue in a cluster or individual form. In addition, NPSi were deposited in mitochondria and the lysosomes, but the microlymphatic vessels were not blocked by NPSi. Pulmonary tissue and pleural membrane in the control groups were not abnormal as shown by transmission electron microscopy.

Pleural and pericardial effusion by sonographic findings

Using thoracic ultrasound, we did not find any pleural effusion on day 1 in any of the groups. On day 3 of administration, pleural effusion was observed in the high-dose group and we suspected fluid in the intermediate group based on sonographic findings. Pleural effusion of most rats was located at the right pleural space, while pericardial effusion was found only in the high-dose group. On day 5, pericardial effusion was also detected in the intermediate-dose group besides pleural effusions. Pleural effusion and pericardial effusion slowly increased to a maximum on days 7–10 and then gradually decreased (Figure 6A and B). On day 14, no water was observed anymore in the intermediate- and high-dose groups, but there were signs of adhesion of pleura. The volume of pleural and pericardial effusion in the intermediate- and high-dose groups was significantly different than that in the saline group and the PA group (rank-sum test, all $P<0.01$). No water in pleural and pericardial cavities was detected in the low-dose group and the control groups. These findings showed that with the rise in concentration of PA/NPSi, pleural effusion was greater and occurred more rapidly, as shown by ultrasonographic qualitative observations.

No apparent morphologic damage of liver and kidney was observed at any time during the study. However, there was ureterectasia and signs of dropsy of kidney in the intermediate- and high-dose groups on days 1 and 3, which then dispersed on days 5–7 after administration of PA/NPSi.

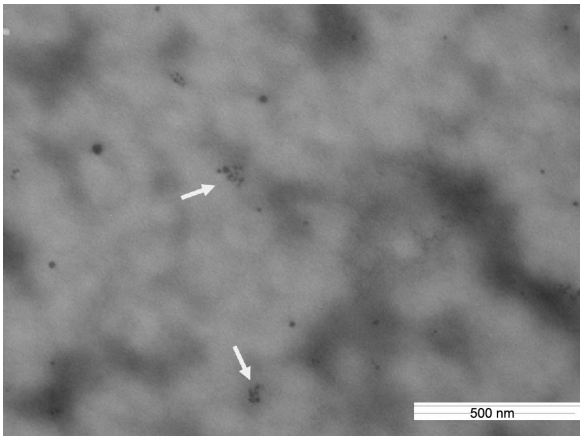

Figure 3 Silica nanoparticles in pleural effusion in a rat.
Note: Silica nanoparticles with clusters are indicated by the arrows.

Thoracic CT images

CT images in both control groups showed no obvious changes, and the texture of the lungs was clear. In the intermediate- and high-dose groups on day 7, there were signs of patching and ambiguity, grinding glass, and local lung consolidation with a rise in PA/NPSi concentrations. On day 14, we still observed an increase in marking of the lungs and signs of grinding glass and pulmonary fibrosis in the intermediate- and high-dose groups, while there were no apparent changes in the low-dose group. Furthermore, in the high-dose group, posteroanterior chest radiography of rats was abnormal, showing blunting of the posterior costodiaphragmatic angle (Figure 7A–F). However, no signs of pleural effusion were observed, which may have been due to an insufficient amount of water.

Discussion

PA/NPSi are a nanocomposite that is widely used in coatings and paints, and this nanocomposite has many special superior properties due to the addition of nanosilica. These properties

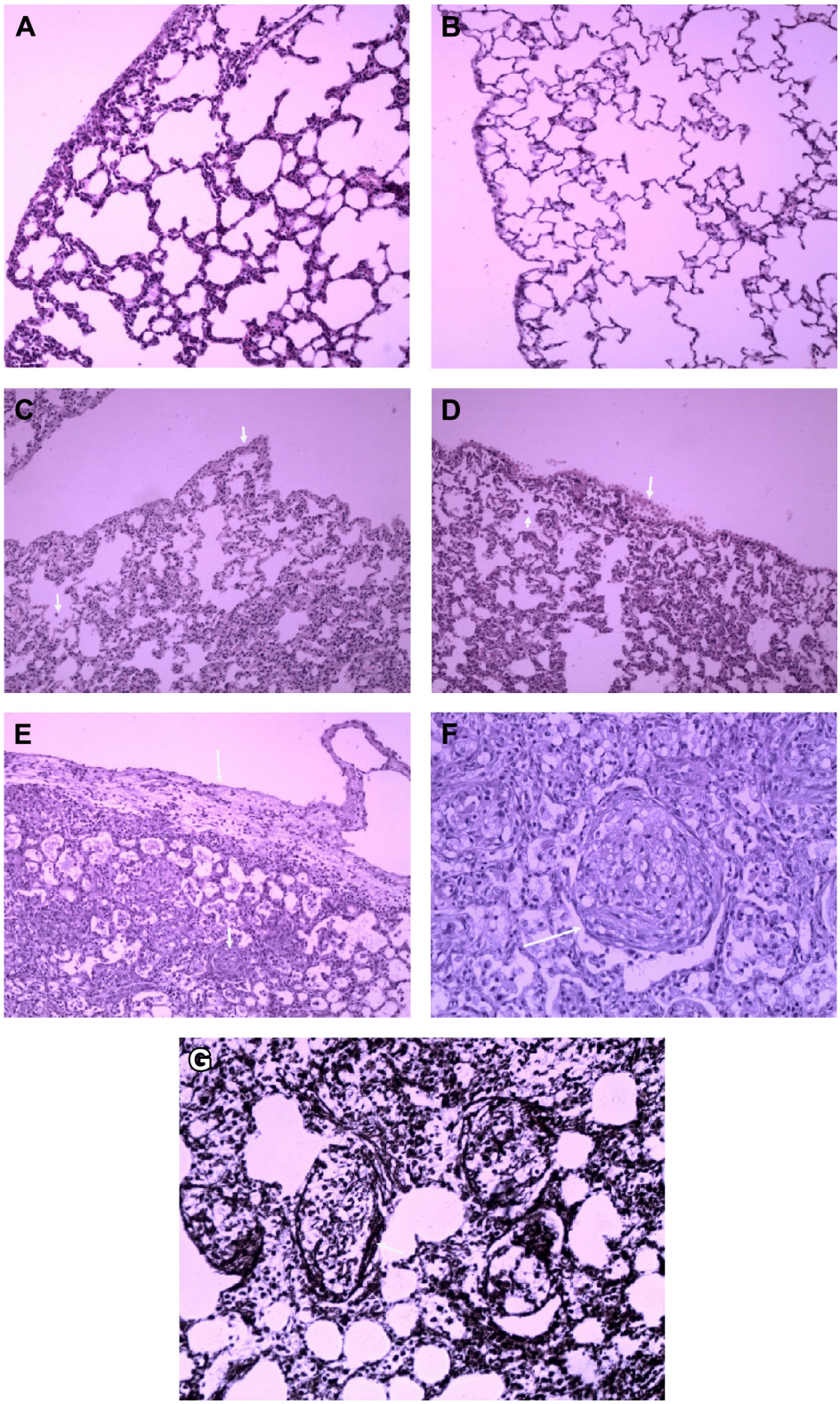

Figure 4 Pathological examinations of pleural membranes and the lungs.
Notes: (**A**, **B**) In the control groups (saline and polyacrylate), there were no changes in appearance and micromorphology of lung and pleural membrane (hematoxylin and eosin ×100). (**C**) Pulmonary image from a rat in the low-dose group on day 7. Slight alveolar septum thickening and lymphocytic infiltrations were observed with slight hyperplasia of mesothelial cells in the visceral pleura (hematoxylin and eosin ×100). (**D**) Pulmonary image from a rat in the intermediate-dose group on day 7, apparent alveolar septum thickening and lymphocytic infiltrations were observed as well as hyperplasia of mesothelial cells in the visceral pleura (hematoxylin and eosin ×100). (**E**, **F**) Pulmonary image from a rat in the high-dose group. Pulmonary epithelial hyperplasia and alveolar septum thickening and granulomas, as well as pleural thickening and lymphocytic infiltrations in the visceral pleura (**E**, hematoxylin and eosin ×100; **F**, hematoxylin and eosin ×200). (**G**) Reticular fiber staining showed that reticular fibers enwrapped granulation tissue demonstrating the structure of granulomas (×200). Edema and lymphocytic infiltrations in the visceral pleura are indicated by the arrows.

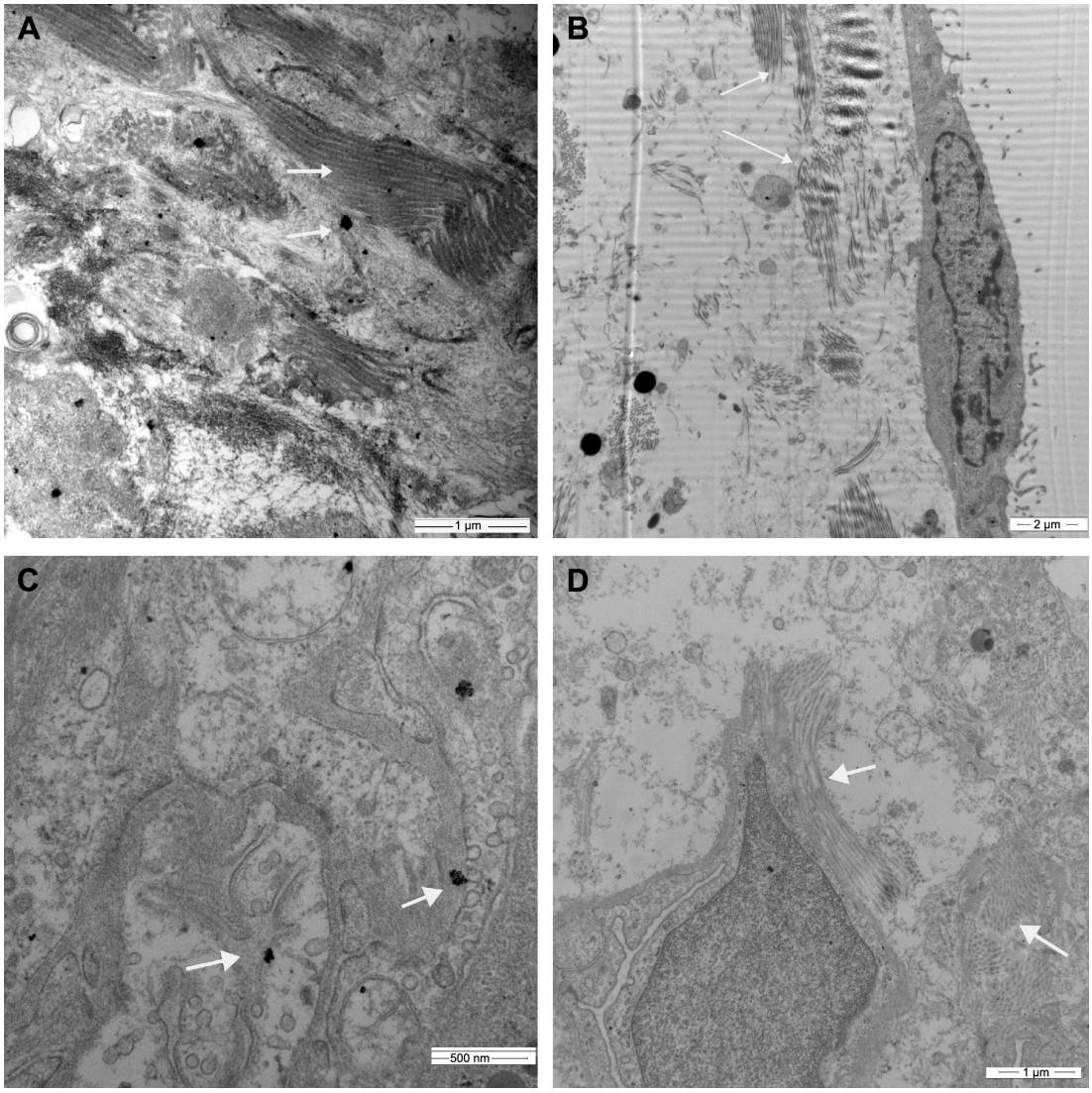

Figure 5 TEM observations of parietal pleural membranes and lungs.
Notes: (**A**, **B**) On day 7, there were a lot of collagen fibers in the lung and the parietal pleural membrane in a rat in the high-dose group with nanoparticles deposited. (**C**, **D**) On day 14, in the low-dose group, a rat's alveolar septum was enlarged, and hyperplasia and slight fibrosis of alveolar interstitium were found with scattered silica nanoparticles. Silica nanoparticles in cluster form are indicated by the arrows.

include enhanced chemical resistance, erosion and abrasion resistance, resistance to UV light, and antifouling properties.[5–7] However, the potential toxicity and their release into the environment have not been well reported. We previously found that a group of patients exposed to PA/NPSi had pleural and pericardial effusion, pulmonary fibrosis, and granuloma, which we suspected were related to their high exposure to PA/NPSi.[9–11] Our present study showed that PA/NPSi caused specific toxicity presenting as pleural and pericardial effusion, fibrosis of lung and pleura, and pulmonary granuloma. These findings are almost identical to the previously reported patients. Our results in turn indicate that the death and injury to workers are closely related to exposure to PA/NPSi.

The main characteristic of our patients was the large amount of water in the pleural and pericardial cavities. Sonography, CT, and dissection of rats showed that PA/NPSi caused pleural and pericardial effusion. Effusion occurred on day 3, gradually rose to a maximum on days 7–10, then slowly decreased and disappeared on day 14. When we administered rats a higher dose of PA/NPSi, pleural effusion was greater and occurred more rapidly. Furthermore, NPSi were also detected in pleural effusions, which is another important finding, similar to that found in patients' pleural effusion.[9,10] Thus, it is not difficult to understand why our patients presented with large pleural effusions, as well as pericardial effusion, after they had been heavily exposed to PA/NPSi.

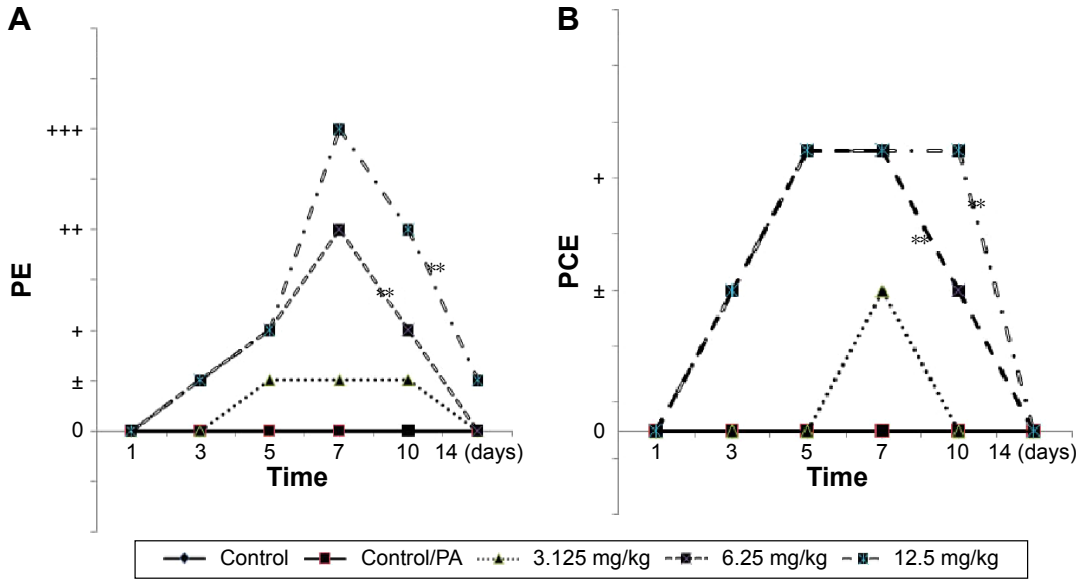

Figure 6 Pleural and pericardial effusion determined by sonographic findings.
Notes: (**A**) Changes in pleural effusion (PE) in different groups. (**B**) Changes in pericardial effusion (PCE). Pleural effusion (**A**) and pericardial (**B**) effusion occurred on day 3 or day 5, gradually rose to a maximum on days 7–10, and then slowly decreased and disappeared on day 14. The volumes of pleural and pericardial effusion in intermediate- and high-dose groups were significantly different from than that in the saline group (rank-sum test, all $^{**}P<0.01$).
Abbreviation: PA, polyacrylate.

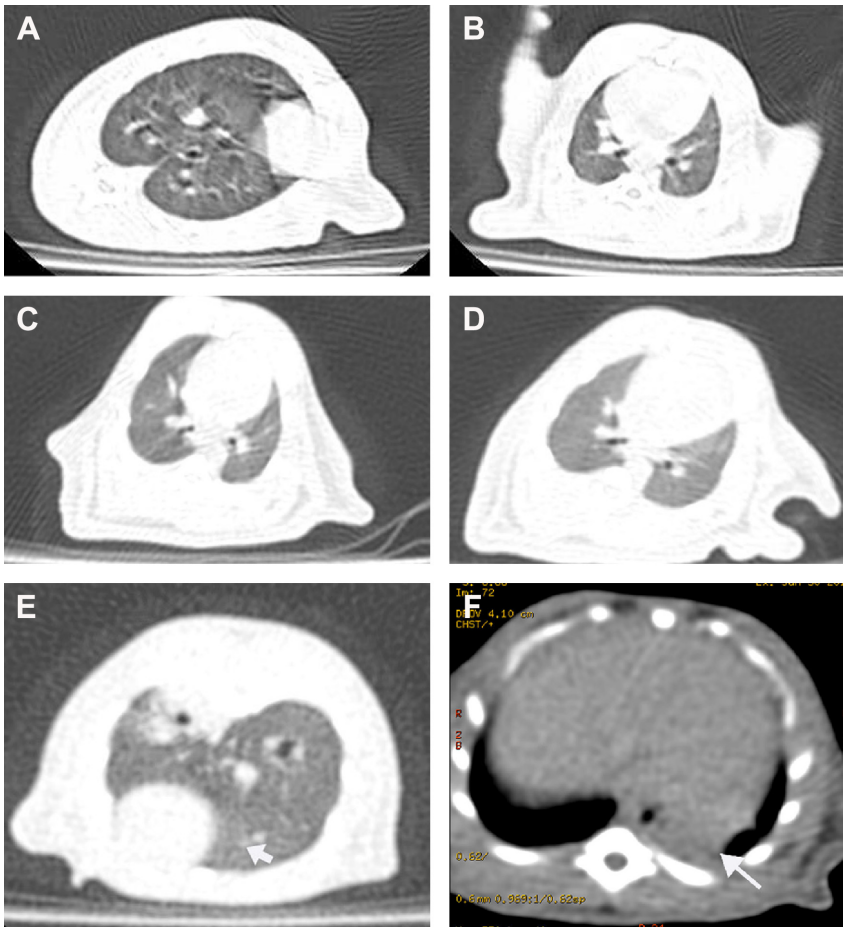

Figure 7 Thoracic CT images of rats.
Notes: (**A**, **B**) Computed tomography (CT) images from the rats in the control groups (saline and polyacrylate), the rats' lung texture is clear. (**C**, **D**) CT images from the rats in the low- and intermediate-dose groups – no pleural effusions were observed. (**E**, **F**) CT images from a rat in the high-dose group show that there is no water in the pleural cavity, but there is blunting of the posterior costodiaphragmatic angle. The arrow represents signs of grinding glass (**E**) and blunting of the posterior costodiaphragmatic angle (**F**).

When intratracheal instillation of the materials that workers used at the workplace was provided to rats at doses of 5–10 mg/kg, pulmonary edema with little water in the pleural cavity on day 1 and ~8–10 mL of water were found on day 7.[13] With administration of a higher dose of materials that workers used, effusion was greater and occurred much more rapidly, which is similar to findings in our study. Additionally, a pathologic examination showed edema of alveoli, an increased amount of alveolar macrophages and interstitial neutrophil infiltration at the early stage, and occurrence of lung fibrosis on day 10.[13] Furthermore, transmission electron microscopy showed damage of cell membrane and mitochondrion at the early stage, and on day 7, there was loss of microvillus and collagen fibers.[13] Our present study showed inflammation in alveolar interstitium, edema of alveolar interstitium at the early stage, and alveolar wall thickening. We also observed hyperplasia and fibrosis of lung and pleura, as well as pulmonary granuloma on day 7. Our present findings are similar to reported results in humans at the workplace, as well as to results in rats that were provided postintratracheal instillation of the materials used at the workplace.[9,10,13]

Toxicity of PA/NPSi in patients and rats is shown by effusion in the pleural and pericardial cavities. Pleural fluid is normally generated from the capillaries of the parietal pleura, it infiltrates the pleural space, and is absorbed by the parietal pleural lymphatics. Pleural fluid may occur and accumulate whenever the volume of pleural fluid formation exceeds that of its reabsorption. The mechanisms that frequently caused pleural effusion include the following: 1) increased pleural fluid formation, possibly because of increased interstitial fluid in the lung, increased permeability of the pleural capillaries, increased intravascular pressure in the pleura, decreased pleural pressure, or decreased serum oncotic pressure and/or 2) decreased pleural fluid absorption, possibly because of obstruction of drainage in the lymphatics or elevation of systemic vascular pressure.[14] PA/NPSi cause pleural effusion in patients and rats, but we did not find any water in the PA only group. This finding indicates that the pleural effusion is related to nanosilica or that nanosilica plays a major role in the formation of pleural effusions. The possible mechanisms, in our opinion, may be as follows.

First, increased interstitial fluid in the lungs because of inflammation and reactive oxygen species (ROS) production may be a possible reason for effusion. Studies have shown that NPSi increase ROS concentrations, cause mitochondrial depolarization, reduce glutathione levels, and induce proinflammatory, inflammatory production both in vivo and in vitro.[15–17] Moreover, nanosilica has been shown to accumulate in the lungs, liver, kidney, gut, bone marrow, and brain in animal experiments and cause multiorgan damage.[17–19] Inflammation and ROS production caused by nanosilica may increase interstitial fluid in the lungs or increase permeability of the pleural capillaries and help to produce more fluid in the pleural cavity.

To mimic conditions in the workplace, PA/NPSi used in the present study were not sterilized and directly administered to the rats. PA/NPSi together with some possible contaminants on the surface of nanosilica particles may contribute to inflammation or ROS production and accelerate the occurrence of the fluid in pleural space. However, we found that pleural effusion occurred on day 3 and was greatest on days 7–10 in rats. Pleural effusion persists for months, and glucocorticoids and antibiotics are not effective in patients.[9] This pleural effusion is difficult to explain just simply by the mechanism of inflammation and ROS production.

Another possible reason for pleural effusion may be related to lymphatic obstruction, as found in asbestos-related benign pleuritis and effusion.[20] The parietal pleural lymphatic system is important in terms of reabsorption of effusion. Lymphatic flow velocity in initial lymphatics under physiological conditions is 2 mm/min,[21] which is much slower than blood flow velocity, and is prone to blockage of the pleural lymphatic stomata. Therefore, an asbestos body can obstruct parietal pleural microlymphatics and cause pleural effusion. Similarly, a large number of NPSi may penetrate the pleural cavity, flow into the microlymphatics, mechanically block the microlymphatics and damage its function of reabsorption, and then cause effusion. Unfortunately, we did not find any obstruction of parietal pleural microlymphatics, possibly because of our single, but not repeated, administration.

The final and most plausible reason for effusion may be nanosilica directly damaging the microlymphatics and affecting lymphangiogenesis and reabsorption of fluid. Microlymphatic vessels are structurally composed of partly overlapping, lymphatic endothelial cells supported by a discontinuous cell adhesion and basement membranes. This structure contributes to high permeability of microlymphatic vessels. Therefore, some immune cells, as well as nanoparticles, can easily enter and exit the lymphatic vessel lumen.[22] Furthermore, nanomaterials have special properties such as lymphatic tropism and lymph tissue-targeting property.[23,24] Because of the aforementioned special properties, nanomaterials such as NPSi have been extensively used as drug carriers, especially in the imaging and treatment

of cancer.[25] However, lymphatic tropism and the lymph tissue-targeting property of nanoparticles may lead to injury of the lymphatic vessels and affect its function.

A previous study showed that silicate nanoparticles effectively inhibit VEGF-induced angiogenesis in vitro and suppress ERK 1/2 activation via inhibition of VEGFR-2 phosphorylation.[26] Additionally, NPSi can inhibit the expression of p-VEGFR2 and p-ERK1/2 and then inhibit the angiogenesis and disturb the heart formation and development.[19] VEGF is the key mediator in pleural effusion formation.[27] Therefore, silica nanoparticles may damage the microlymphatics and affect lymphangiogenesis and its function of reabsorption of fluid by influencing VEGF and its receptors and promote formation of pleural effusion. Similarly, pericardial effusion may occur in a manner similar to pleural effusion by some mechanisms.

The exact mechanisms of pleural and pericardial effusion related to PA/NPSi remain unknown. Damage of the microlymphatic system and its function by nanosilica may be the most likely reason for the presence of effusion. Further studies are required to focus on the special clinical characteristics and possible mechanisms of pleural effusion.

Currently, there is little research on the toxicity of nanomaterials on humans and much less research on the toxicity of PA/NPSi. Our present study showed that exposure to PA/NPSi could cause toxicity as shown by pleural effusion, pulmonary fibrosis, and granuloma in rats, similar to exposed workers. Our study highlights the urgent need and importance for safety practice in the development of nanoscience and nano-products, as well as awareness of toxicity of PA/NPSi. Protocols may include regulations for occupational health and safety and industrial hygiene guidelines in the field of nanotechnology, medical surveillance, and effective personal protective equipment. Furthermore, complete assessment of the potential risks and effects of nanomaterials' release on human health and the environment is essential before they enter the market. If products contain nanomaterials, it should be clearly stated or labeled because the suspected injury related to nanomaterials clinically are observed among consumers, not nanomaterial-producing workers. Nanomaterials should be considered hazardous until proven otherwise.

Conclusion

Our study shows that exposure to PA/NPSi results in toxicity as shown by pleural effusion/pericardial effusion, pulmonary fibrosis, and granuloma in rats, similar to exposed workers. This finding indicates that particular symptoms of the reported workers are closely related to the exposure to PA/NPSi.[9] This highlights the urgent need and importance of nanosafety and awareness of release of nanoparticles into the environment, as well as the toxicity of PA/NPSi.

Acknowledgments

The present study was funded by the National Natural Science Foundation of China (grant numbers 81172614 and 81441089). We thank Professor Wang Rugang and Yu Guixin (Beijing Center for Disease Prevention and Control, People's Republic of China) for performing hematology analysis and blood biochemical assays. We also thank Dr Zhao Hongying (Department of Pathology, Beijing Chaoyang Hospital) for assistance with pathological analysis, Professor Zhang Dongfeng (Department of Epidemiology and Health Statistics, Qingdao University Medical College, People's Republic of China) for statistical analysis, and Professor Dai Wei and Han Yehua (Peking Union Medical College, Chinese Academy of Medical Sciences, People's Republic of China) for transmission electron microscopy analysis.

Disclosure

The authors report no conflicts of interest in this work.

References

1. Li S, Meng Lin M, Toprak MS, Kim do K, Muhammed M. Nanocomposites of polymer and inorganic nanoparticles for optical and magnetic applications. *Nano Rev*. 2010;1.
2. Zaragoza J, Babhadiashar N, O'Brien V, et al. Experimental investigation of mechanical and thermal properties of silica nanoparticle-reinforced poly(acrylamide) nanocomposite hydrogels. *PLoS One*. 2015;10(8):e0136293.
3. Vellayappan MV, Balaji A, Subramanian AP, et al. Multifaceted prospects of nanocomposites for cardiovascular grafts and stents. *Int J Nanomedicine*. 2015;10:2785–2803.
4. Budnyak TM, Pylypchuk IV, Tertykh VA, Yanovska ES, Kolodynska D. Synthesis and adsorption properties of chitosan-silica nanocomposite prepared by sol-gel method. *Nanoscale Res Lett*. 2015;10:87.
5. Luna-Xavier JL, Guyot A, Bourgeat-Lami E. Synthesis and characterization of silica/poly (methyl methacrylate) nanocomposite latex particles through emulsion polymerization using a cationic azo initiator. *J Colloid Interface Sci*. 2002;250(1):82–92.
6. Ma JZ, Hu J, Zhang ZJ. Polyacrylate/silica nanocomposite materials prepared by sol–gel process. *Eur Polymer J*. 2007;43(10):4169–4177.
7. Cui XJ, Zhong SL, Yan J, Wang CL, Zhang HT, Wang HY. Synthesis and characterization of core–shell SiO2-fluorinated polyacrylate nanocomposite latex particles containing fluorine in the shell. *Colloids Surf A*: *Physicochem Eng Aspects*. 2010;360(1–3):41–46.
8. Zhou S, Wu L, Sun J, Shen W. The change of the properties of acrylic-based polyurethane via addition of nano-silica. *Prog Org Coat*. 2002;45:33–42.
9. Song Y, Li X, Du X. Exposure to nanoparticles is related to pleural effusion, pulmonary fibrosis and granuloma. *Eur Respir J*. 2009;34(3):559–567.
10. Song Y, Li X, Wang L, et al. Nanomaterials in humans: identification, characteristics, and potential damage. *Toxicol Pathol*. 2011;39(5):841–849.

11. Song Y, Tang S. Nanoexposure, unusual diseases, and new health and safety concerns. *ScientificWorldJournal*. 2011;11:1821–1828.
12. Huang Y, Chen G, Zou Q, Wu Li. [Preparation and form study of nano-SiO_2 combined water-borne acrylic resin]. *China Paint*. 2005;20(1). Chinese.
13. Ma ZF, Li XX, Wang YW, Wang DX, Zheng YX, Sun X. [Development of animal model for lung injury in rats caused by unknown polymer via intratracheal instillation]. *Zhonghua Lao Dong Wei Sheng Zhi Ye Bing Za Zhi*. 2012;30(1):52–58. Chinese.
14. Thomas R, Jenkins S, Eastwood PR, Lee YC, Singh B. Physiology of breathlessness associated with pleural effusions. *Curr Opin Pulm Med*. 2015;21(4):338–345.
15. Skuland T, Ovrevik J, Låg M, Refsnes M. Role of size and surface area for pro-inflammatory responses to silica nanoparticles in epithelial lung cells: importance of exposure conditions. *Toxicol In Vitro*. 2014;28(2):146–155.
16. Brown DM, Kanase N, Gaiser B, Johnston H, Stone V. Inflammation and gene expression in the rat lung after instillation of silica nanoparticles: effect of size, dispersion medium and particle surface charge. *Toxicol Lett*. 2014;224(1):147–156.
17. Duan J, Yu Y, Li Y, et al. Low-dose exposure of silica nanoparticles induces cardiac dysfunction via neutrophil-mediated inflammation and cardiac contraction in zebrafish embryos. *Nanotoxicology*. 2015;9:1–11.
18. Kaewamatawong T, Shimada A, Okajima M, et al. Acute and subacute pulmonary toxicity of low dose of ultrafine colloidal silica particles in mice after intratracheal instillation. *Toxicol Pathol*. 2006;34(7):958–965.
19. Duan J, Yu Y, Li Y, Yu Y, Sun Z. Cardiovascular toxicity evaluation of silica nanoparticles in endothelial cells and zebra fish model. *Biomaterials*. 2013;34(23):5853–5862.
20. Müller KM, Schmitz I, Konstantinidis K. Black spots of the parietal pleura: morphology and formal pathogenesis. *Respiration*. 2002;69(3):261–267.
21. Miserocchi G. Mechanisms controlling the volume of pleural fluid and extravascular lung water. *Eur Respir Rev*. 2009;18(114):244–252.
22. Tammela T, Alitalo K. Lymphangiogenesis: molecular mechanisms and future promise. *Cell*. 2010;140(4):460–476.
23. Hou M, Chen Z, Li L, Wang P, Qie M. Studies on the lymphatic tropism and lymph cells apoptosis of cisplatin-nano carbon suspension in the rats. *Zhonghua Fu Chan Ke Za Zhi*. 2014;49(11):847–851.
24. Cho HY, Lee YB. Nano-sized drug delivery systems for lymphatic delivery. *J Nanosci Nanotechnol*. 2014;14(1):868–880.
25. Nazir S, Hussain T, Ayub A, Rashid U, MacRobert AJ. Nanomaterials in combating cancer: therapeutic applications and developments. *Nanomedicine*. 2014;10(1):19–34.
26. Jo DH, Kim JH, Yu YS, Lee TG, Kim JH. Antiangiogenic effect of silicate nanoparticle on retinal neovascularization induced by vascular endothelial growth factor. *Nanomedicine*. 2012;8(5):784–791.
27. Grove CS, Lee YC. Vascular endothelial growth factor: the key mediator in pleural effusion formation. *Curr Opin Pulm Med*. 2002;8(4):294–301.